Supplemental Material to:

Zhengzhi Zou, Zhongyu Yuan, Qiongxia Zhang, Zijie Long, Jinna Chen, Zhiping Tang, Yuliang Zhu, Shupeng Chen, Jie Xu, Min Yan, Jing Wang and Quentin Liu

Aurora kinase A inhibition-induced autophagy triggers drug resistance in breast cancer cells

Autophagy 2012; 8(12)
http://dx.doi.org/10.4161/auto.22110

www.landesbioscience.com/journals/autophagy/article/22110

A

	AURKB (H)	AURKB (L)	*P* value
SQSTM1 (H)	69	125	0.436
SQSTM1 (L)	7	18	
Total (T)	76	143	
Percentage (H/T)	35%	65%	

Sperman's correlation=0.053, *P* value=0.436

B

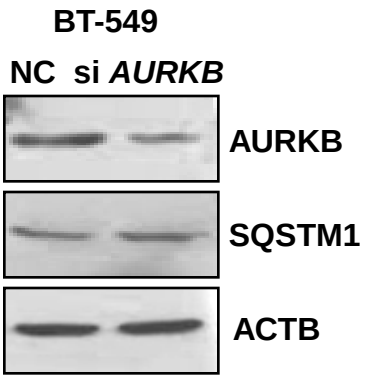

Figure S1. AURKB was not correlated with autophagy-associated protein SQSTM1 expression in breast cancer.

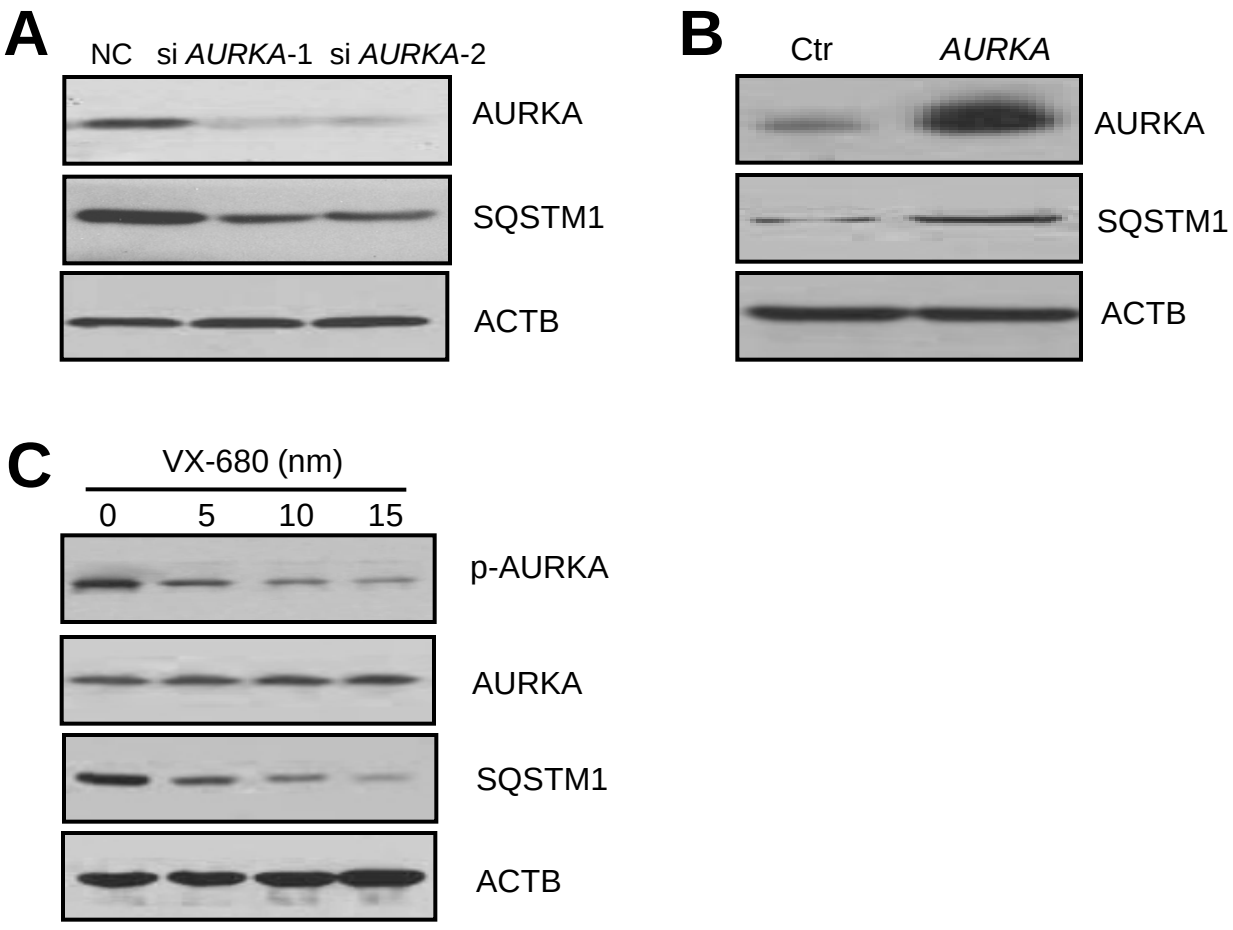

Figure S2. AURKA correlated with autophagy-associated protein SQSTM1 expression in ZR-75-1 cells.

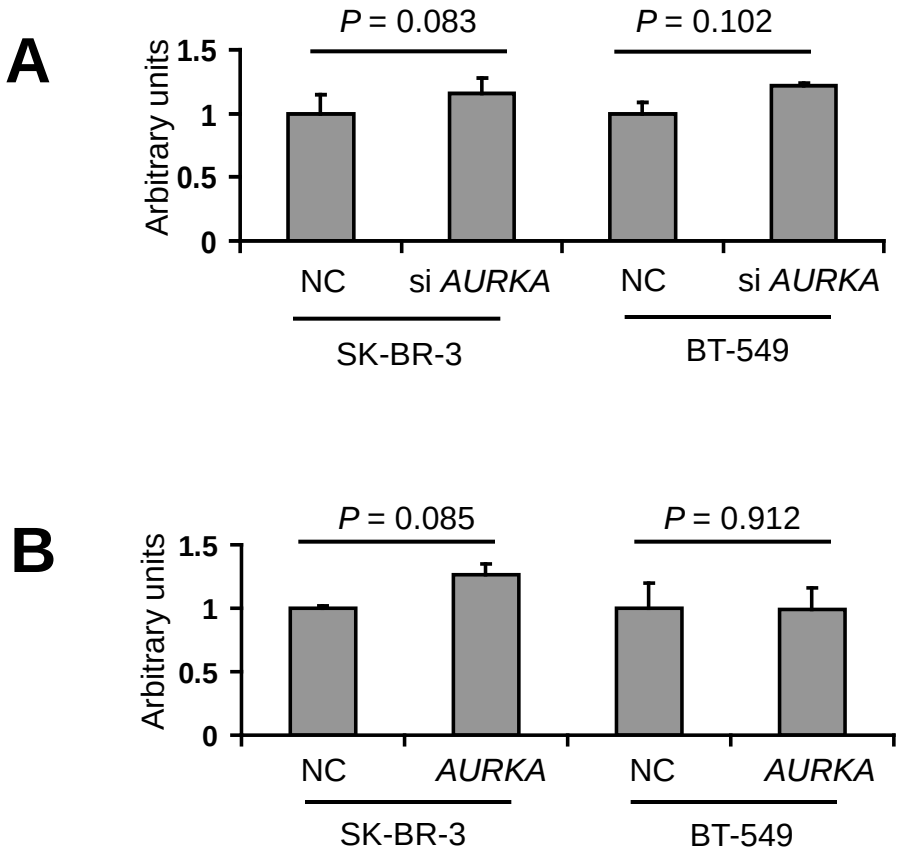

Figure S3. AURKA regulated autophagy-associated protein SQSTM1 expression independent of mRNA level.

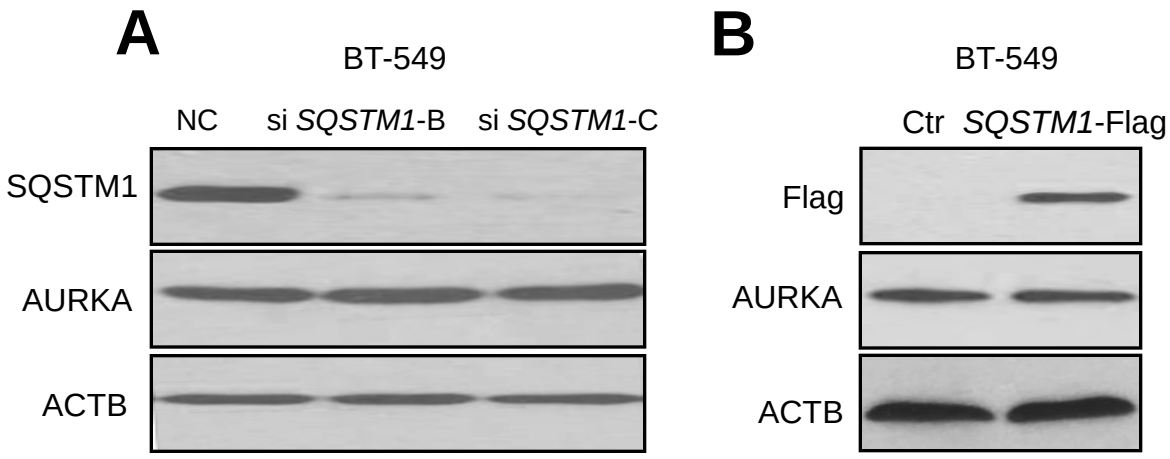

Figure S4. SQSTM1 failed to influence the expression of AURKA.

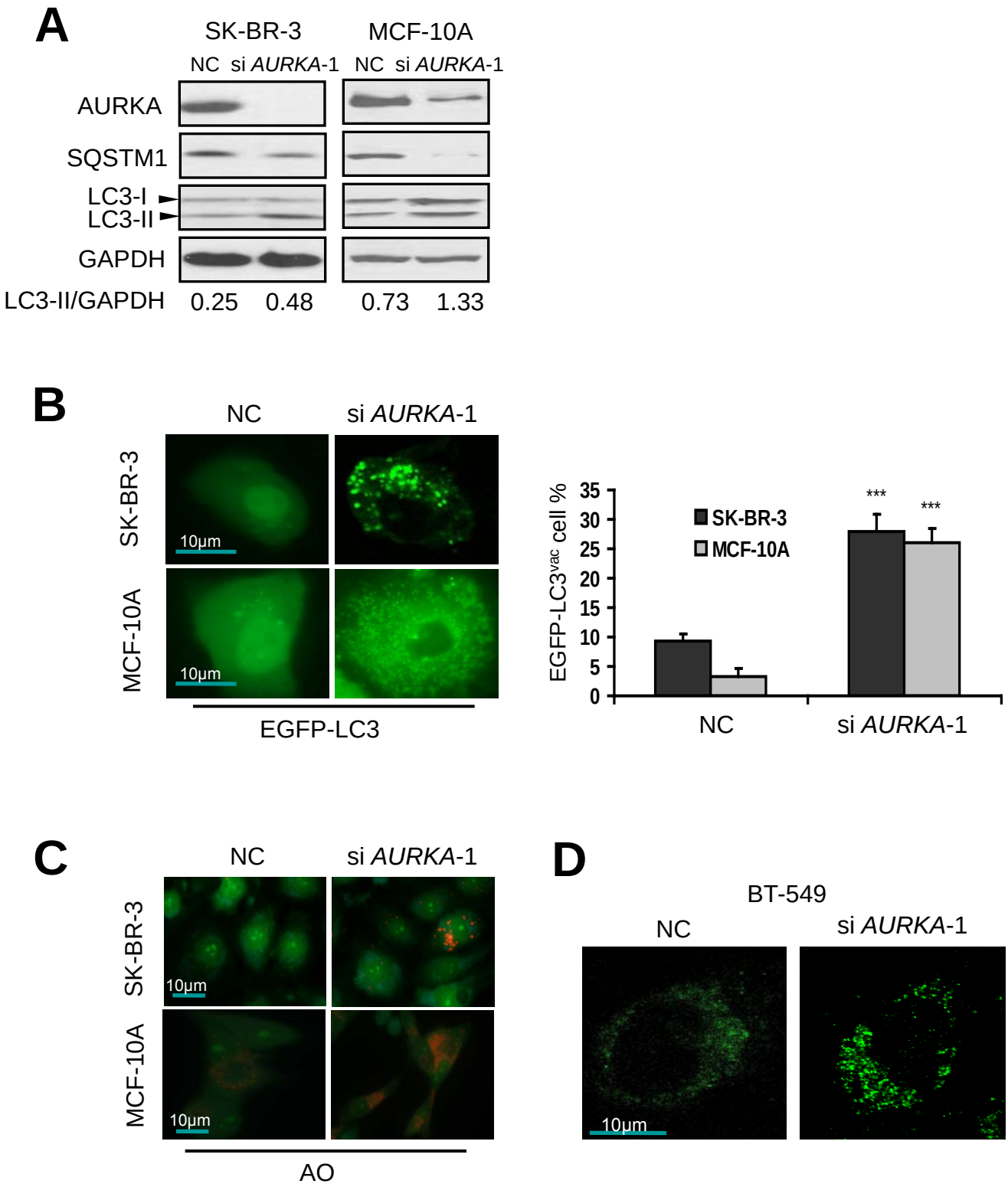

Figure S5. Depletion of AURKA induced autophagy.

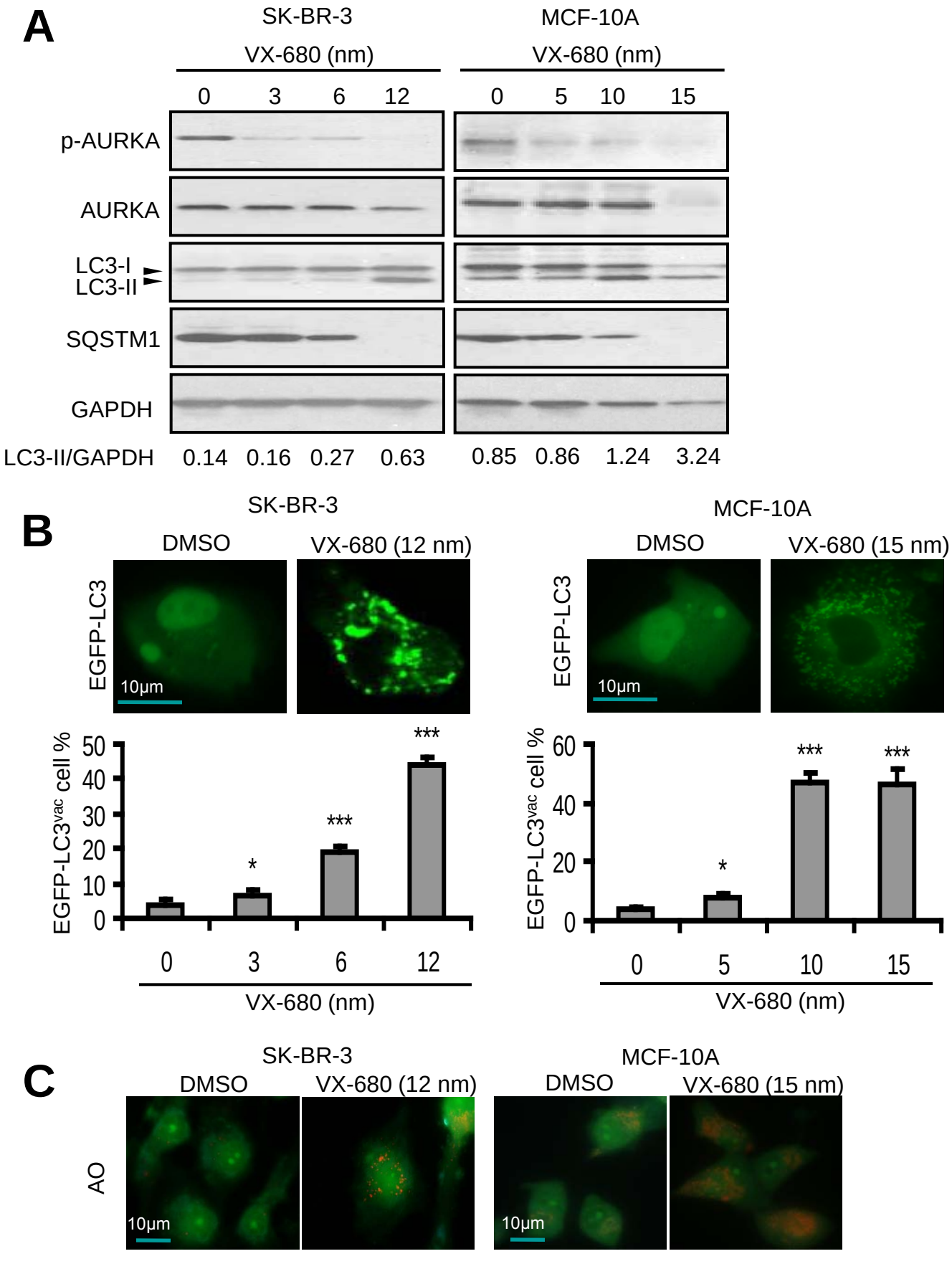

Figure S6. Inhibition of AURKA induced autophagy.

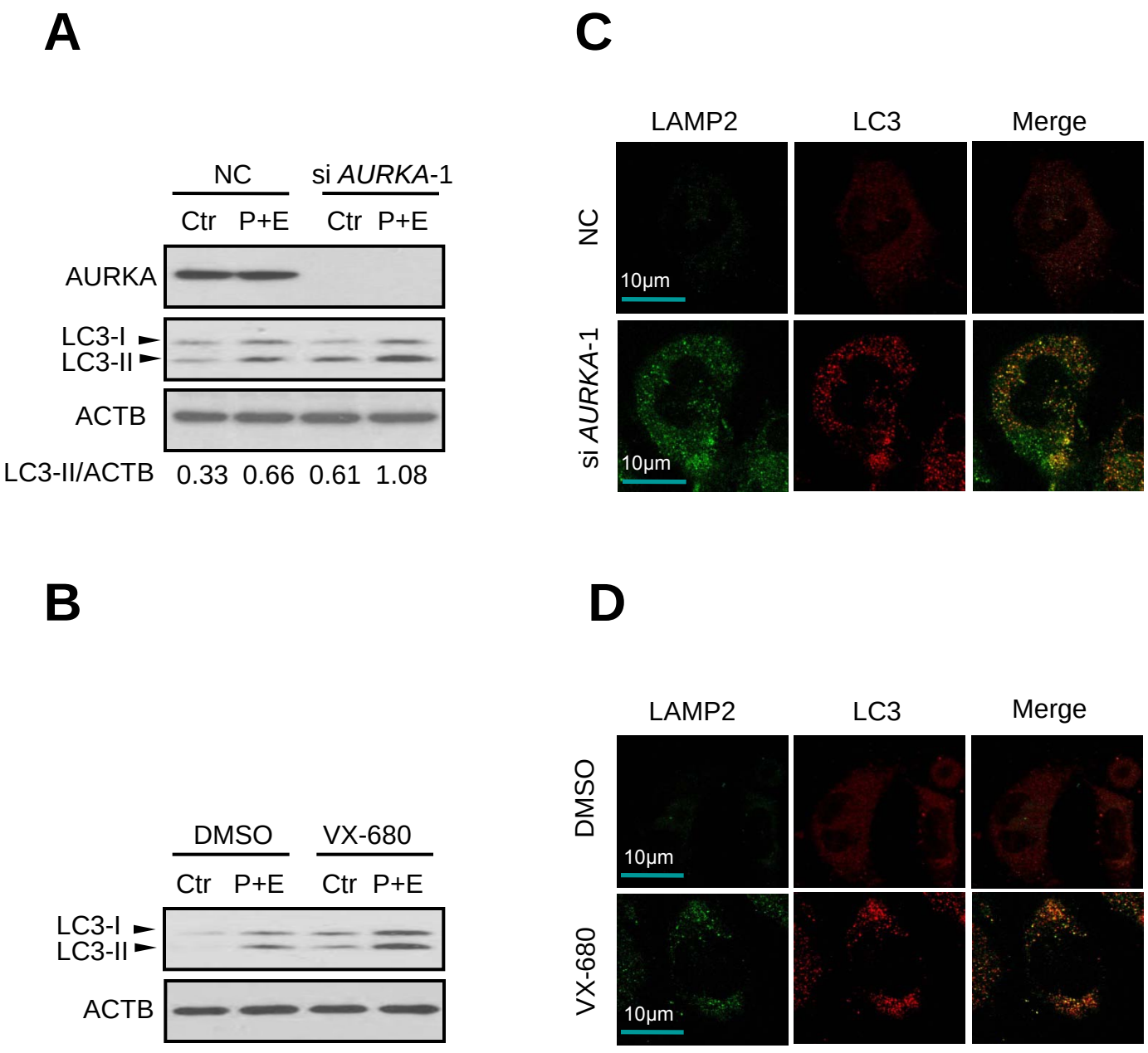

Figure S7. Depletion or inhibition of AURKA failed to block autophagosome-lysosome fusion.

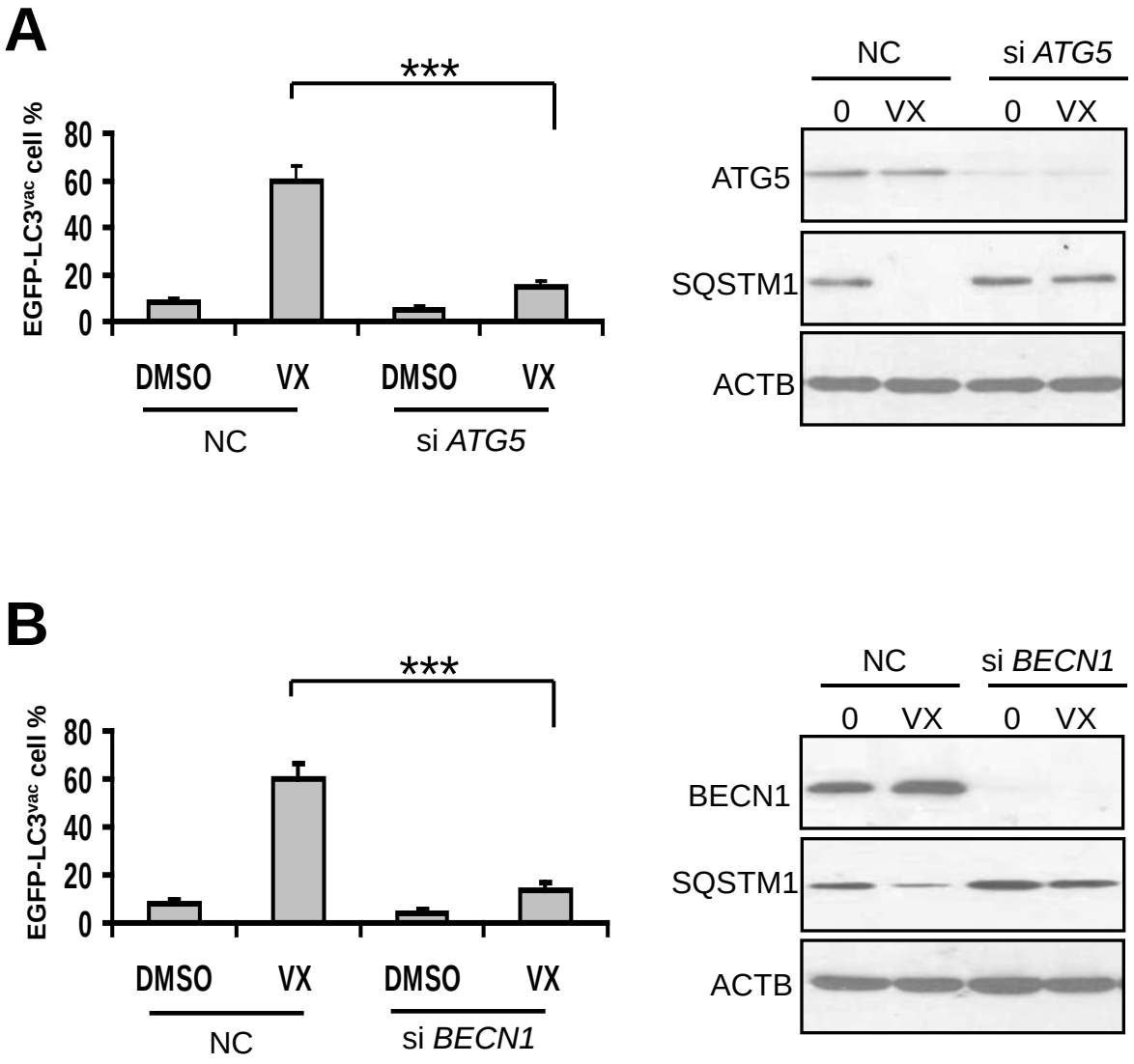

Figure S8. Autophagy induction by inhibition of AURKA was associated with the canonical pathway.

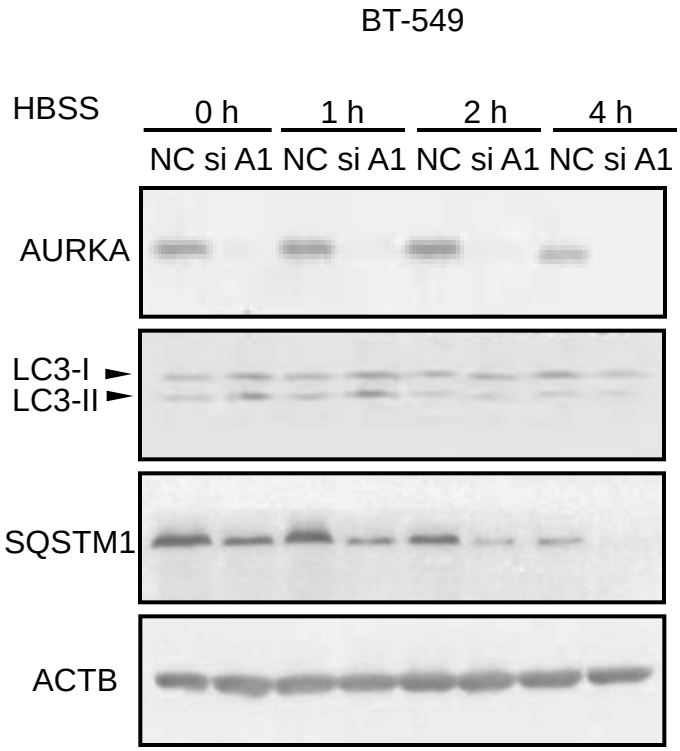

Figure S9. Downregulation of AURKA induced autophagy under conditions of nutrient deprivation.

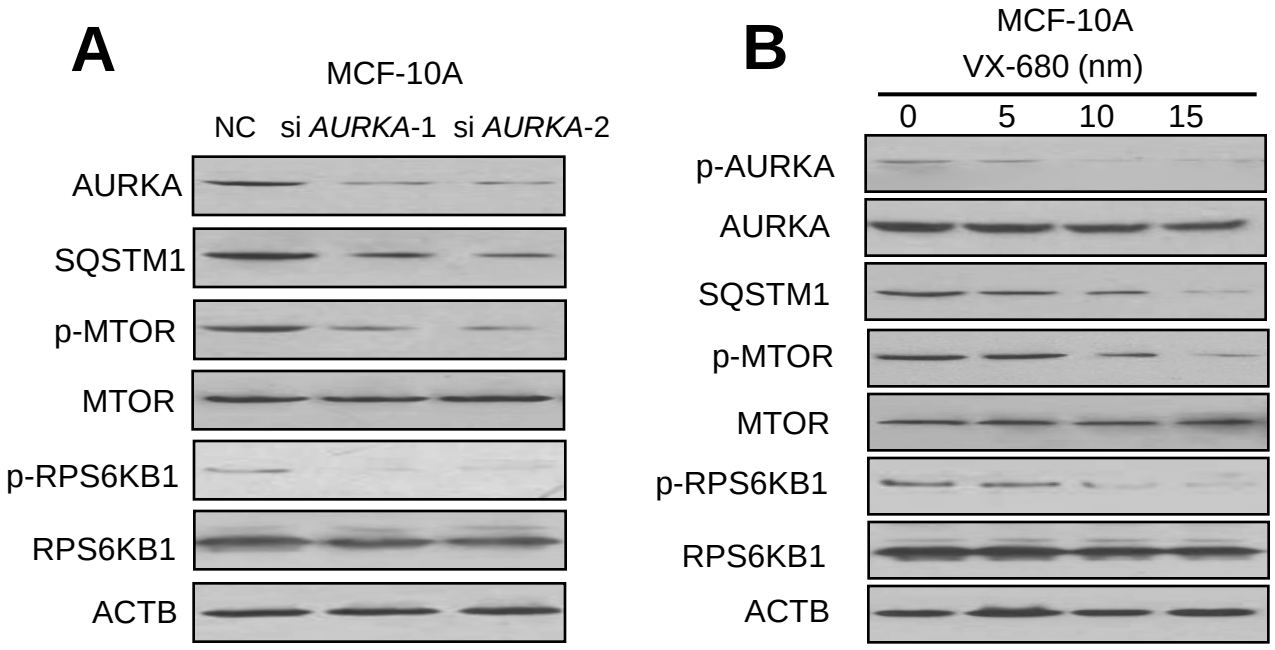

Figure S10. AURKA-suppressed autophagy was associated with MTOR activation in MCF-10A cells.

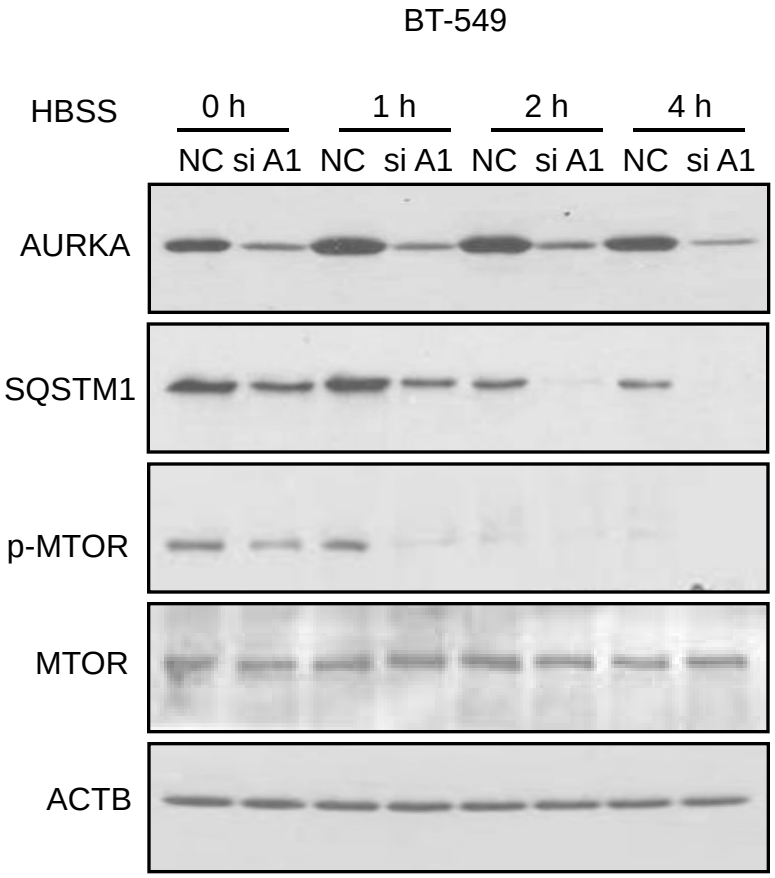

Figure S11. Downregulation of AURKA induced autophagy associated with MTOR activation.

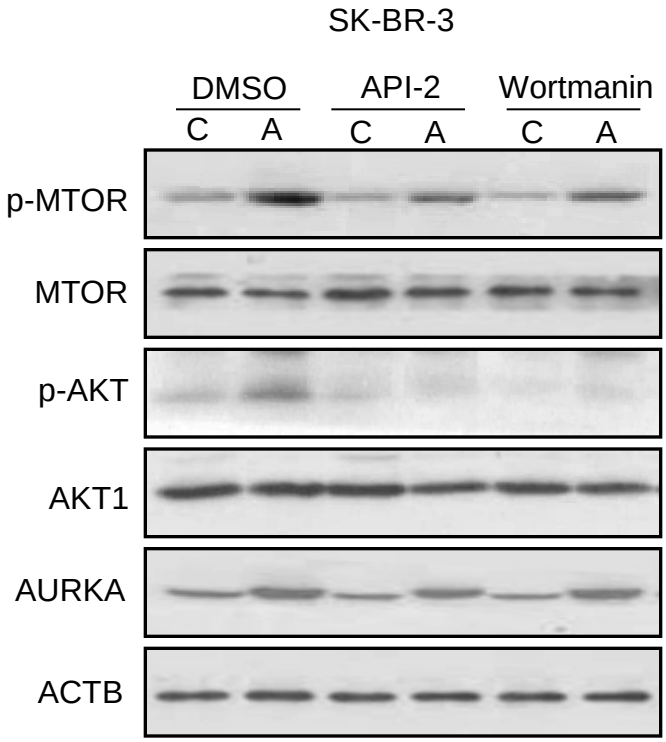

Figure S12. AURKA regulated MTOR independently of the PtdIns3K-AKT1 pathway.

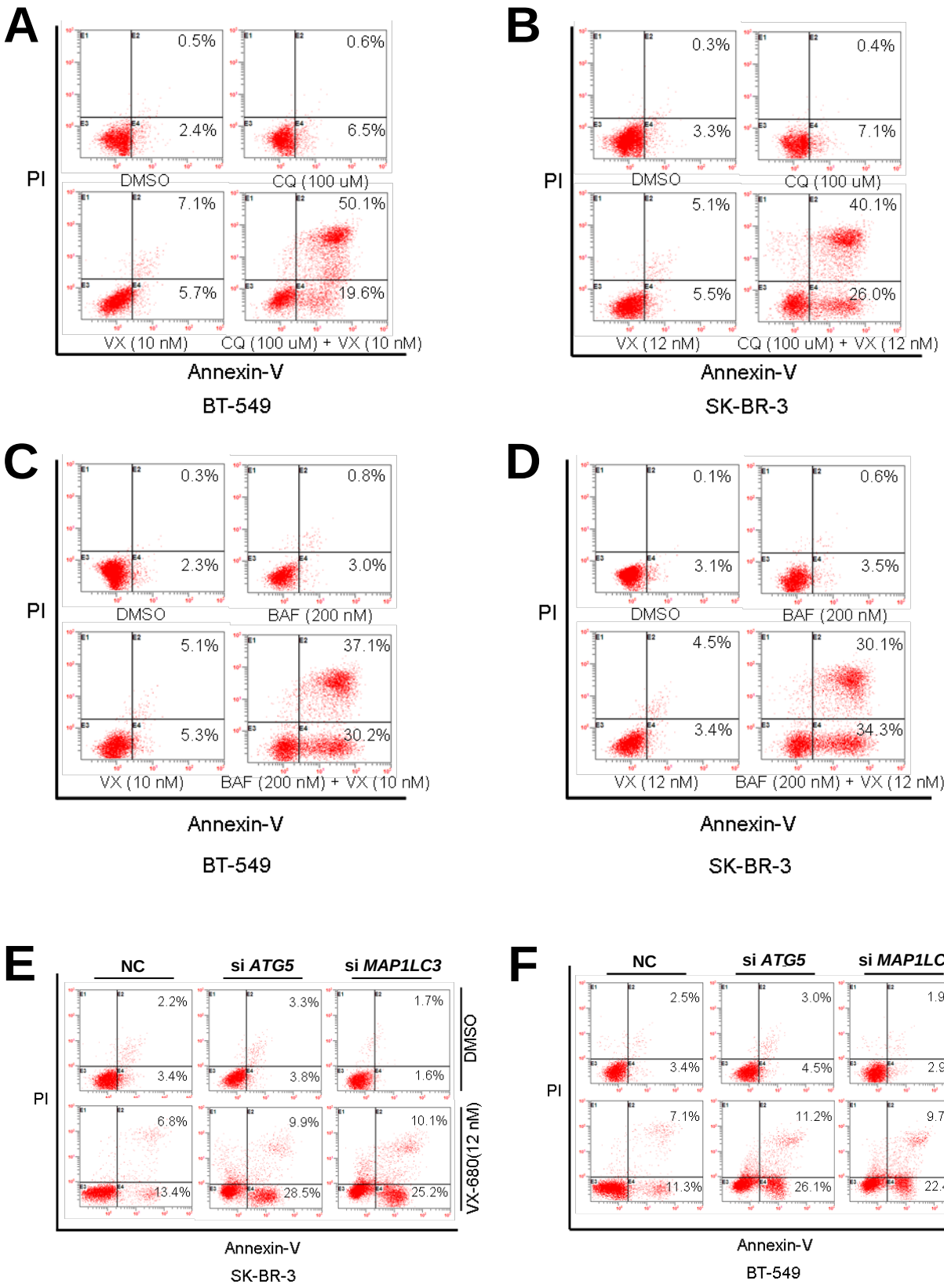

Figure S13. Inhibition of autophagy enhanced VX-680-induced apoptosis in breast cancer cells.

Supplementary figure legends

Figure S1. AURKB was not correlated with autophagy-associated protein SQSTM1 expression in breast cancer. (A) The results were calculated on the basis of analyses performed using 219 breast cancer tissue samples. The relationship between AURKB and SQSTM1 expression was compared using Spearman's correlation coefficient. (B) BT-549 cells were treated with 100 nM *AURKB* siRNA (si *AURKB*) and negative control (NC) siRNA for 24 h respectively. Cell lysates were subjected to western blot analysis with the indicated antibodies.

Figure S2. AURKA correlated with autophagy-associated protein SQSTM1 expression in ZR-75-1 cells. (A) ZR-75-1 cells were treated with 100 nM *AURKA*-1 siRNA (si *AURKA*-1), *AURKA*-2 siRNA (si *AURKA*-2) and NC siRNA for 24 h respectively, and then cell lysates were subjected to western blot analysis with the indicated antibodies. (B) Control (Ctr) and AURKA-overexpressing cells were lysed and assayed by western blot similarly. (C) Cells were treated with increasing doses of VX-680 for 24 h, and then cell lysates were subjected to western blot analysis.

Figure S3. AURKA regulated autophagy-associated protein SQSTM1 expression independent of mRNA level. (A) SK-BR-3 and BT-549 cells were treated with 100 nM *AURKA* siRNA (si *AURKA*-1) and negative control (NC) siRNA for 24 h respectively. *SQSTM1* mRNA levels were then determined by real-time quantitative PCR. (B) *SQSTM1* mRNA levels were determined by real-time quantitative PCR in control (Ctr) and AURKA-overexpressing (AURKA) cells. Results are the mean ± SD of triplicates.

Figure S4. SQSTM1 failed to influence the expression of AURKA. (A) BT-549 cells were treated with 100 nM *SQSTM1*-B siRNA, *SQSTM1*-C siRNA and NC siRNA for 24 h respectively, and then cell lysates were subjected to western blot analysis with indicated antibodies. (B) Control (Ctr) and SQSTM1-overexpressing cells were lysed and subjected to western blot assays similarly.

Figure S5. Depletion of AURKA induced autophagy. (A) SK-BR-3 and MCF-10A cells were treated with 100 nM *AURKA*-1 siRNA and NC siRNA for 24 h respectively, and then cell lysates were subjected to western blot analysis with indicated antibodies. LC3-II and GAPDH were quantified using Image J software. (B) SK-BR-3 and MCF-10A cells were transfected with EGFP-LC3. At 24 h post-transfection, cells were transfected with *AURKA*-1 siRNA and NC siRNA. After additional 24 h post-transfection, the localization of EGFP-LC3 in transfected cells was examined by confocal microscopy (magnification × 1000). The percentage of cells showing accumulation of EGFP-LC3 in puncta (EGFP-LC3^{vac}) was quantified. A minimum of 100 EGFP-LC3-transfected cells were counted. Results are the mean ± SD of triplicates. ***, $P < 0.001$, compared with control. (C) SK-BR-3 and MCF-10A cells were treated with 100 nM *AURKA*-1 siRNA and NC siRNA for 24 h respectively. Cells were stained with acridine orange (AO) and examined by fluorescence microscopy (magnification × 400). Large orange puncta were considered to be visualized acidic vesicular organelles (AVOs). (D) BT-549 cells were treated with 100 nM *AURKA*-1 siRNA and NC siRNA for 24 h respectively, then immunostained with LC-3 antibody and FITC-labelled secondary antibody, and

visualized under a confocal microscope.

Figure S6. Inhibition of AURKA induced autophagy. (A) SK-BR-3 and MCF-10A cells were treated with increasing dose of VX-680 for 24 h, and then cell lysates were subjected to western blot analysis. LC3-II and GAPDH were quantified using Image J software. (B) SK-BR-3 and MCF-10A cells were transfected with EGFP-LC3. At 24 h post-transfection, cells were treated with increasing doses of VX-680 for 24 h. Localization of EGFP-LC3 in transfected cells was examined by confocal microscopy (magnification × 1000), the percentage of cells showing accumulation of EGFP-LC3 in puncta (EGFP-LC3^{vac}) was quantified. A minimum of 100 EGFP-LC3–transfected cells were counted. Results are the mean ± SD of triplicates. *, $P < 0.05$; ***, $P < 0.001$, compared with controls. (C) SK-BR-3 and MCF-10A cells were treated with 12 nM and 15 nM VX-680 for 24 h respectively. Cells were stained with acridine orange (AO) and examined by fluorescence microscopy (magnification × 400). Large orange puncta were considered to be visualized acidic vesicular organelles (AVOs).

Figure S7. Depletion or inhibition of AURKA failed to block autophagosome-lysosome fusion. (A) BT-549 cells were treated with 100 nM *AURKA*-1 siRNA and NC siRNA for 24 h respectively, and then cells were treated with or without 10 μg/ml pepstatin A (P) and 10 μg/ml E64-d (E) for additional 12 h. Cell lysates were subjected to western blot analysis. LC3-II and ACTB were quantified using Image J software. (B) BT-549 cells were treated with 5 nM VX-680 and DMSO for 24 h, and then cells were treated with or without 10 μg/ml pepstatin A (P) and 10 μg/ml E64-d (E) for

additional 12 h. Cell lysates were analyzed by western blot with antibodies against LC3 and ACTB. Densitometry analysis of LC3-II levels relative to ACTB was performed using Image J software. (C) BT-549 cells were treated with 100 nM *AURKA*-1 siRNA and NC siRNA for 24 h respectively, and then immunostained for LAMP2 and LC3 to observe the colocalization between LC3 and LAMP2. Representative confocal microphotographs are shown together with the profiles of colocalization. (D) BT-549 cells were treated using 5 nM VX-680 and DMSO for 24 h respectively and then immunostained for LAMP2 and LC3 to observe the colocalization between LC3 and LAMP2. Representative confocal microphotographs were shown together with the profiles of colocalization.

Figure S8. Autophagy induction by inhibition of AURKA was associated with the canonical pathway. (A and B) BT-549 cells were transfected with EGFP-LC3. At 8 h post-transfection, cells were transfected with *ATG5* or *BECN1* siRNA. After additional 24 h post-transfection, cells were treated with 10 nM of VX-680 for 24 h. The percentage of cells showing accumulation of EGFP-LC3 in puncta (EGFP-LC3^{vac}) was quantified. A minimum of 100 EGFP-LC3-transfected cells were counted. Results are the mean ± SD of triplicates. ***, $P < 0.001$, compared with control. ATG5, BECN1 and SQSTM1 expression level were detected by western blot (right panel).

Figure S9. Downregulation of AURKA induced autophagy under conditions of nutrient deprivation. BT-549 cells were treated with NC siRNA and *AURKA*-1 siRNA (si A1) for 24 h. Thereafter cells were subjected to HBSS starvation for the indicated time

intervals. Cell lysates were subjected to western blot assays with the indicated antibodies.

Figure S10. AURKA-suppressed autophagy was associated with MTOR activation in MCF-10A cells. (A) MCF-10A Cells were treated with 100 nM *AURKA*-1 siRNA, *AURKA*-2 siRNA and NC siRNA for 24 h respectively, and then cell lysates were subjected to western blot analysis. (B) MCF-10A cells were treated with increasing dose of VX-680 for 24 h, and then cell lysates were analyzed by western blot assays.

Figure S11. Downregulation of AURKA induced autophagy associated with MTOR activation. BT-549 cells were treated with NC siRNA and *AURKA*-1 siRNA (si A1) for 24 h. Thereafter cells were subjected to HBSS starvation for the indicated time intervals. Cell lysates were analyzed by western blot assays.

Figure S12. AURKA regulated MTOR independently of the PtdIns3K-AKT1 pathway.

Control (C) and AURKA-overexpressing (A) SK-BR-3 cells were treated with DMSO, 15 μM API-2 and 10 μM wortmanin for 24 h respectively. Cell lysates were assayed by western blot.

Figure S13. Inhibition of autophagy enhanced VX-680-induced apoptosis in breast cancer cells. BT-549 **(**A and C) and SK-BR-3 (B and D) cells were pretreated with 100 μM chloroquine (CQ) and 200 nM bafilomycin A_1 (BAF) for 1 h, and then BT-549 and SK-BR-3 cells were treated with 10 nM and 12 nM VX-680 (VX) for additional 24 h

respectively, cell apoptosis was measured using an Annexin V-FITC/PI staining assay. SK-BR-3 **(**E) and BT-549 (F) cells were transfected with 100nM NC siRNA, *ATG5* siRNA and *MAP1LC3* siRNA respectively. For 24 h later, SK-BR-3 and BT-549 were treated with 12 nM and 10 nM VX-680 for 24 h respectively, cell apoptosis was measured using the Annexin V-FITC/PI staining assay.

Supplementary methods

Plasmid construction

The plasmids encoding human (Aurora kinase A) *AURKA* and *SQSTM1* with flag tags were generated by PCR amplification. *AURKA* was subcloned into the Mlu I and BamH I sites of PLVPT[1]. *SQSTM1* was subcloned into the XhoI and HindIII sites of pLVPT.

Generation of stable transfection cell lines

MCF-10A, BT-549, ZR-75-1 and SK-BR-3 cell lines with vector and stable overexpression of AURKA (Flag tagged) were constructed using a lentivirus vector (pLVPT). BT-549 cell lines with vector and stable SQSTM1 overexpression (Flag tagged) were constructed with a lentivirus vector (pLVPT).

Tissue microarray construction

Tissue microarray was used to detect the expression of SQSTM1, AURKA and AURKB by immunohistochemistry. In brief, the formalin-fixed, paraffin-embedded tissue blocks and the corresponding histological Hematoxylin and eosin stained slides were overlaid for tissue microarray sampling. In view of tumor heterogeneity, triplicate

0.6-μm-diameter cylinders of tissue were punched from selected tumor areas of individual donor tissue blocks and re-embedded into a recipient paraffin block at defined positions, using a tissue arraying instrument (Beecher Instruments, Silver Spring, MD). The tissue microarray block contained 341 breast cancer samples. Subsequently, multiple sections (5 μm thick) were cut from the tissue microarray block and mounted on microscope slides. Hematoxylin and eosin staining was used to one section from the tissue array to confirm that the punches contained tumor region.

Immunohistochemical evaluation

The immunoreactivity for SQSTM1, AURKA and AURKB was scored through a semi-quantitative method by evaluating the number of positive tumor cells over the total number of tumor cells. We scored the staining intensity of SQSTM1, AURKA and AURKB as following: negative (score 0), weak (score 1), moderate (score 2), and strong (score 3). Staining extent was graded into five levels according to the percentage of elevated staining cells in the field: negative (score 0), 1-25% (score 1), 26-50% (score 2), 51-75% (score 3), 75-100% (score 4). Immunoreactivity staining was evaluated and scored by two independent pathologists blinded to clinical follow-up data. Their conclusions were in agreement in 85% of the cases, which showed this scoring method was highly reproducible.

Selection of Cutoff Score

Receiver operating characteristic (ROC) curve analysis was performed to determine cutoff score for breast cancer "high expression" by using the 0, 1-criterion.[2, 3] The cutoff value for AURKA in breast cancer was determined as 4.[1] At the SQSTM1 and AURKB

scores, the sensitivity and specificity for each outcome were plotted, thus generating various ROC curves. The scores were decided as the cutoff value, which was closest to the point with both maximum specificity and sensitivity. In this study, the cutoff scores for AURKB and SQSTM1 were determined as 4 and 5 respectively. Breast cancer designated as low expression of SQSTM1, AURKA and AURKB were those with the scores below or equal to the cutoff value. Conversely breast cancer with high expression of SQSTM1, AURKA and AURKB were those with scores above the value. For using ROC curve analysis, the clinical and pathologic characteristics were dichotomized: clinical stage (I-II versus III-IV), cancer progression (Yes versus No), T classification (T1-T2 versus T3-T4), N classification (N0-N1 versus N2-N3), distant metastasis (M0 versus M1), and survival status.[4]

References:

1. Wang LH, Xiang J, Yan M, Zhang Y, Zhao Y, Yue CF, Xu J, Zheng FM, Chen JN, Kang Z, Chen TS, Xing D, Liu Q. The mitotic kinase Aurora-A induces mammary cell migration and breast cancer metastasis by activating the Cofilin-F-actin pathway. Cancer Res 2010; 70:9118-28.
2. Goin JE, Haberman JD. Comments on the logistic function in ROC analysis: applications to breast cancer detection. Methods Inf Med 1982; 21:26-30.
3. Zlobec I, Steele R, Terracciano L, Jass JR, Lugli A. Selecting immunohistochemical cut-off scores for novel biomarkers of progression and survival in colorectal cancer. J Clin Pathol 2007; 60:1112-6.
4. Zhu W, Cai MY, Tong ZT, Dong SS, Mai SJ, Liao YJ, Bian XW, Lin MC, Kung HF, Zeng YX, Guan XY, Xie D. Overexpression of EIF5A2 promotes colorectal carcinoma cell aggressiveness by upregulating MTA1 through C-myc to induce epithelial-mesenchymaltransition. Gut 2012; 61:562-75.